© 2016. Published by The Company of Biologists Ltd | Journal of Cell Science (2016) 129, 2261-2272 doi:10.1242/jcs.183889

RESEARCH ARTICLE

PAX5 interacts with RIP2 to promote NF-κB activation and drug-resistance in B-lymphoproliferative disorders

Dong Wang[1,2,3], Jingyu Chen[1,2,3], Rui Li[1,2,3], Guolin Wu[4], Zimin Sun[4], Zhitao Wang[5], Zhimin Zhai[5], Fang Fang[1,2,3], Yugang Guo[1,2,3], Yongjun Zhong[1,2,3], Ming Jiang[1,2,3], Huan Xu[1,2,3], Minhua Chen[1,2,3], Guodong Shen[1,2,3], Jie Sun[1,2,3], Bailing Yan[6], Chundong Yu[3], Zhigang Tian[1,2,3] and Weihua Xiao[1,2,3,*]

ABSTRACT

Paired box protein 5 (PAX5) plays a lineage determination role in B-cell development. However, high expression of PAX5 has been also found in various malignant diseases, including B-lymphoproliferative disorders (B-LPDs), but its functions and mechanisms in these diseases are still unclear. Here, we show that PAX5 induces drug resistance through association and activation of receptor-interacting serine/threonine-protein kinase 2 (RIP2; also known as RIPK2), and subsequent activation of NF-κB signaling and anti-apoptosis gene expression in B-lymphoproliferative cells. Furthermore, PAX5 is able to interact with RIP1 and RIP3, modulating both RIP1-mediated TNFR and RIP2-mediated NOD1 and NOD2 pathways. Our findings describe a new function of PAX5 in regulating RIP1 and RIP2 activation, which is at least involved in chemotherapeutic drug resistance in B-LPDs.

KEY WORDS: Drug resistance, B-lymphoproliferative disorders, NF-κB, PAX5, RIP2

INTRODUCTION

B-lymphoproliferative disorders (B-LPDs) are characterized by abnormal B-lymphocyte proliferation and monoclonal lymphocytosis, encompassing B-cell lymphomas, multiple myeloma and leukemia, which are caused by virus infection and gene mutation. PAX5 maintains B-cell lineage development through transcriptional regulation (Cobaleda et al., 2007). Deregulation of PAX5 has been associated with various types of tumorigenesis (Cazzaniga et al., 2001; Kanteti et al., 2009; Kozmik et al., 1995; Kubetzko et al., 2004; Stuart et al., 1995), especially in B-cell malignancies, such as lymphoma and lymphocytic leukemia (Cobaleda et al., 2007; Krenacs et al., 1998). PAX5 expression is prevalent in B-LPDs, but not in plasma B-cell malignancies (Dong et al., 2008). In addition, about 30% of multiple myeloma cases have been found to be accompanied by PAX5 expression (Lin et al., 2004). CD20 and PAX5 have been used as a biomarker to classify a subgroup of multiple myeloma (Zhan et al., 2006). It suggests that PAX5 expression is relevant to B-LPDs pathogenesis.

[1]Key Laboratory of Innate Immunity and Chronic Disease of CAS, School of Life Sciences, University of Science and Technology of China, Hefei, Anhui 230027, China. [2]Hefei National Laboratory for Physical Sciences at Microscale, Hefei, Anhui 230027, China. [3]Innovation Center for Cell Signaling Network, School of Life Sciences, Xiamen University, Xiamen, Fujian 361005, China. [4]Department of Hematology, Anhui Provincial Hospital, 17 Lujiang Road, Hefei, Anhui Province 230001, China. [5]Department of Hematology, The Second Hospital of Anhui Medical University, 678 Furong Road, Hefei, Anhui Province 230601, China. [6]Emergency Department, the First Hospital of Jilin University, Changchun 130021, China.

*Author for correspondence (xiaow@ustc.edu.cn)

W.X., 0000-0001-9102-6326

Received 27 November 2015; Accepted 11 April 2016

Bortezomib has been proven to be effective for the treatment of multiple myeloma and plasma cell leukemia, which are PAX5-negative B-LPDs (Esparis-Ogando et al., 2005; Utecht and Kolesar, 2008; Zhan et al., 2006). However, the effect of Bortezomib on PAX5-positive B-cell lymphomas and leukemia is limited (Goy et al., 2005; Liu et al., 2009; Strauss et al., 2006). Therefore, Bortezomib has different effects in the treatment of B-LPDs, which might be attributed to the activation of anti-apoptotic pathways. Therefore, the question remains as to the relationship between PAX5 expression and the pathways of drug-resistance in B-LPDs.

The nuclear factor-kappa B (NF-κB) pathway is constitutively activated in clinical samples and cell lines of B-LPDs (Jost and Ruland, 2007; Keller et al., 2006). NF-κB activation decreases apoptosis and drug-sensitivity of B-LPDs, and has been identified as a crucial element in drug resistance (Jost and Ruland, 2007; Keller et al., 2006; Li et al., 2008; Mitsiades, 2002; Strauss et al., 2006). However, the relationship between PAX5 expression and high intracellular NF-κB activity, as well as drug-resistance in PAX5-positive B-LPDs cells remains unexplored.

In this study, we demonstrate that PAX5-positive primary cells, including CD34-positive leukemia cells and CD138-positive multiple myeloma cells from peripheral blood and bone marrow of affected individuals, respectively, are more resistant to drug-induced apoptosis compared with PAX5-negative primary cells. PAX5 directly interacts with RIP2 (also known as RIPK2) and significantly enhances phosphorylation of RIP2 at Ser176, which promotes drug-triggered NF-κB activation and drug resistance. Our findings describe a new function of PAX5 and signaling pathway of PAX5-regulated NF-κB activation, suggesting that PAX5 participates in the NF-κB activation and drug-resistance of PAX5-positive B-LPDs, and that it could be used as a potential target for therapy in B-LPDs.

RESULTS

PAX5-positive cells are more resistant to chemotherapy drugs

It has been reported that PAX5 is expressed in most B-LPDs (Dong et al., 2008). Moreover, a large proportion of B-LPDs show a limited response to chemotherapy. To explore the relevance of PAX5 for drug resistance in B-LPDs, the PAX5-positive IM9 cell line was used as a representative PAX5-positive malignant B-cell line (Brien et al., 2007; Chu et al., 2014; Davis et al., 2010; Min et al., 2009; Shimizu et al., 2006). U266 and RPMI8226 cell lines were employed as PAX5-null multiple myeloma cell lines, and the Daudi cell line was used as a PAX5-positive Burkitt's-lymphoma-derived B-lymphoblast representative (Fig. 1A). Drug-induced apoptosis assays showed that, in comparison with U266 and RPMI8226 cells, IM9 and Daudi cells exhibited a strong resistance to Bortezomib-induced apoptosis (Fig. 1B). It has been reported that

Journal of Cell Science (2016) 129, 2261-2272 doi:10.1242/jcs.183889

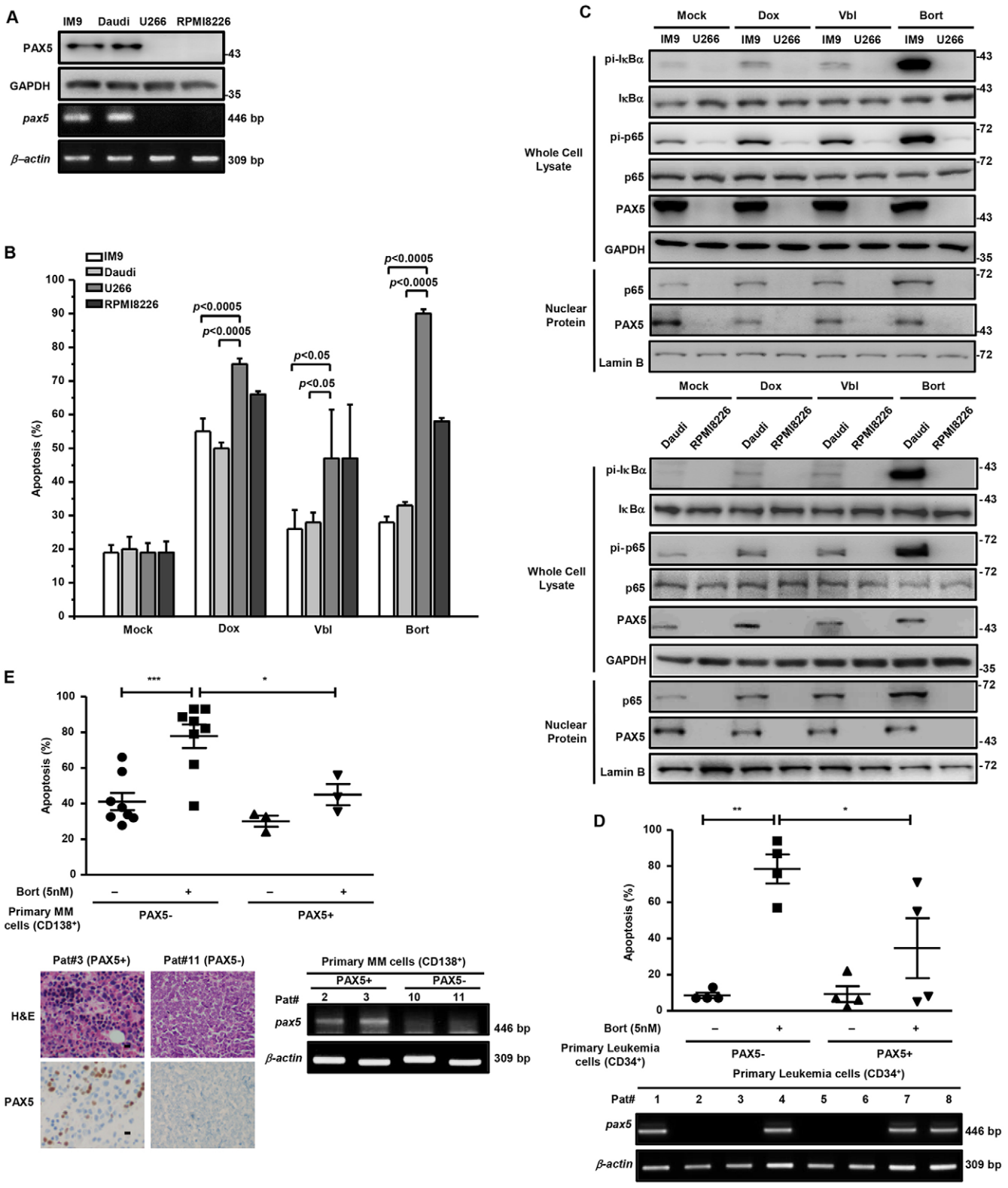

Fig. 1. Drug resistance and NF-κB activation in PAX5-positive and PAX5-negative cell lines and primary cells. (A) Expression of PAX5 in IM9, Daudi, U266 and RPMI8226 cells was examined by western blotting (upper panel) and RT-PCR analysis (lower panel). (B) Fluorescence-activated cell sorting (FACS) assay for apoptosis after culturing cells in the presence or absence of Bortezomib (Bort) (10 nM), Doxorubicin (Dox) (1 µg/ml) or Vinblastine (Vbl) (1 µg/ml) for 30 h. *P*-values, two-tailed Student's *t*-test. (C) IM9 and U266 cells, Daudi and RPMI8226 cells were cultured with or without Bortezomib (20 nM), Doxorubicin (10 µg/ml) or Vinblastine (10 µg/ml) for 4 h after serum starvation for 48 h. NF-κB activation and nuclear p65 were examined by western blotting. Apoptosis in primary CD34-positive leukemia cells (D) and CD138-positive multiple myeloma (MM) cells (E) was measured after culturing cells in the presence or absence of Bortezomib (5 nM) for 30 h. Apoptosis (%) includes both Annexin-V$^+$ PI$^+$ and Annexin-V$^+$ PI$^-$ cells. PI, propidium iodide. PAX5 expression was examined by using immunohistochemistry and RT-PCR analyses. Scale bar: 10 µm. One-way ANOVA was used. **P*<0.05; ***P*<0.005; ****P*<0.0005. Error bars, ±s.e.m.; data are representative of three independent experiments. Pat#, patient number.

Journal of Cell Science (2016) 129, 2261-2272 doi:10.1242/jcs.183889

various drugs can trigger NF-κB signaling, which can lead to drug-resistance (Hideshima et al., 2009; Pahl, 1999). Doxorubicin, Bortezomib and Vinblastine induced NF-κB activation and p65 (also known as RelA) nuclear translocation in IM9 and Daudi cells, but not in U266 and RPMI8226 cells (Fig. 1C). In addition, two out of four PAX5-positive CD34-positive primary leukemia cell types and all three PAX5-positive CD138-positive primary multiple myeloma cells showed resistance to Bortezomib-induced apoptosis, whereas almost all PAX5-negative primary leukemia and multiple myeloma cells showed good responses to Bortezomib treatment (Fig. 1D and E), indicating PAX5-positive cells were more resistant to Bortezomib than PAX5-negative cells. These data indicate that PAX5 is involved in drug-induced apoptosis, in which, drug-induced NF-κB activation might also play a role.

PAX5 enhances drug-induced RIP2 and NF-κB activation

NF-κB activation has been reported largely in association with progression and drug resistance of B-LPDs (Jost and Ruland, 2007; Keller et al., 2006; Li et al., 2008; Mitsiades, 2002; Xiang et al., 2011). Bortezomib has been demonstrated to activate the canonical NF-κB pathway in multiple myeloma cells through RIP2, which prompted us to evaluate whether PAX5 affects drug-induced NF-κB and RIP2 activation that results in drug resistance. Two stable *PAX5*-knockdown IM9 cell lines were established in which different sequences of the PAX5-coding gene had been targeted using small hairpin (sh)RNAs (called IM9-shPAX5-1 and IM9-shPAX5-2), both of which showed effective PAX5 suppression (Fig. 2A). The IM9-shPAX5-2 cell line with higher PAX5 silencing efficiency was used for subsequent studies. Additionally, expression of the PAX5 target gene CD19 (Kozmik et al., 1992) was significantly decreased in IM9-shPAX5 cells, further confirming PAX5 downregulation in IM9-shPAX5 cells (Fig. 2B). Fig. 2C showed that *PAX5* knockdown reduced Doxorubicin, Bortezomib and Vinblastine-induced RIP2 and NF-κB activation in IM9 cells. Also, drug-induced NF-κB activation was enhanced in PAX5-expressing U266 and RPMI8226 cells (Fig. 2D). These data suggest that PAX5 expression is positively related to drug-induced RIP2 and NF-κB activation.

PAX5 induces drug resistance by promoting RIP2 and NF-κB activation

Chemotherapy drugs frequently activate NF-κB signaling, which prevents apoptosis. We examined whether PAX5-enhanced NF-κB activation was associated with resistance to Doxorubicin-, Bortezomib- and Vinblastine-induced death. As shown in Fig. 3A, IM9 cells expressing a control shRNA (IM9-Crl) showed less drug-induced apoptosis compared to IM9-shPAX5 cells. A low dosage of BAY11-7082 (5 nM), which specifically inhibited NF-κB activation and induced low levels of cell apoptosis (Keller et al., 2000) (Fig. 3A; Fig. S1), eliminated the differences in susceptibility to Bortezomib- and Vinblastine-induced apoptosis between IM9-Crl and IM9-shPAX5 cells, but not to Doxorubicin-induced apoptosis (Fig. 3A). Overexpression of PAX5 in U266 and RPMI8226 cells led to a strong elevation of drug resistance, especially resistance to Bortezomib (Fig. 3B). In addition, *RIP2* knockdown in IM9 cells caused a dramatic increase of Bortezomib-triggered apoptosis, but only moderate augmentation of Vinblastine- and Doxorubicin-induced apoptosis (Fig. 3C). Similarly, the selective RIP2 inhibitor SB 203580, but not the RIP1 inhibitor Necrostatin-1 (Degterev et al., 2013) nor the RIP3 inhibitor Dabrafenib (Li et al., 2014), was able to significantly increase Bortezomib-induced apoptosis in IM9 and PAX5-expressing RPMI8226 cells (Fig. 3D). Furthermore, only SB 203580 decreased Bortezomib-induced activation of RIP2 and NF-κB in IM9 cells (Fig. 3F). The same results were obtained after employing selective shRNAs targeting RIP1, RIP2 and RIP3 (Fig. 3E and G). These results suggest that RIP2 plays a dominant role in Bortezomib resistance in B-LPDs cells. The RIP-family of proteins comprises seven members sharing the highly homologous common kinase domain (Zhang et al., 2010). RIP2 was the most highly expressed RIP-family member expressed in IM9 cells, whereas RIP1 and RIP3 exhibited relatively lower expression levels in IM9 cells (Fig. S2), which might reveal the crucial role of RIP2 in Bortezomib resistance in IM9 cells.

PAX5 and RIP2 affect tumor formation and susceptibility to Bortezomib *in vivo*

To further confirm the previous results *in vivo*, a tumor xenograft model was used. As shown in Fig. 4A, downregulation of PAX5 and RIP2 (shRIP2) restrained IM9 tumor growth. Additionally, Bortezomib treatment led to a further reduction in growth of IM9-shPAX5 and IM9-shRIP2 tumors. Moreover, Bortezomib-induced activation of caspase7 and caspase 9 was significantly increased in IM9-shPAX5 and IM9-shRIP2 tumors (Fig. 4B). Additionally, more terminal deoxynucleotidyl transferase dUTP nick-end labeling (TUNEL)-positive cells and fewer proliferating cell nuclear antigen (PCNA)-positive cells were found in Bortezomib-treated IM9-shPAX5 and IM9-shRIP2 tumors than in IM9-Crl tumors (Fig. 4C).

All together, these results demonstrate that PAX5 and RIP2 are both involved in drug-triggered NF-κB activation and lead to drug resistance in B-LPDs, particularly upon treatment with Bortezomib. The data also suggest that interplay between PAX5 and RIP2 activation plays a possible role in cell drug resistance.

PAX5 interacts with RIP2 to participate in the NOD pathway

We next examined how the nuclear transcription factor PAX5 affects activation of RIP2 in the cytoplasm. Previous studies have never shown the link between PAX5 and NF-κB-associated proteins (Pridans et al., 2008). Therefore, we investigated the subcellular distribution of PAX5 and RIP2 in Bortezomib-treated IM9 and Daudi cells. The results showed that there was more PAX5 in the cytoplasm than in the nucleus after Bortezomib treatment (Fig. 5A). Analysis of protein interactions using co-immunoprecipitation showed that PAX5 interacted with RIP2 as well as with RIP1 and RIP3 but not with other NF-κB-associated proteins in unstimulated IM9 and Daudi cells (Fig. 5B). As shown in Fig. 5C, Bortezomib treatment substantially enhanced the interaction between PAX5 and RIP2, but not the binding of PAX5 to RIP1 or RIP3. To further demonstrate the interaction between PAX5 and RIP2, pulldown assays using the glutathione S-transferase (GST) tag were performed (constructs are detailed in Fig. 5D), and they revealed that the RIP2 kinase domain (construct GST–RA) and RIP2 lacking the CARD domain (construct GST–RB) interacted with full-length PAX5 protein. Only the PAX5 that lacked the paired domain (construct GST–PB) could interact with the full-length RIP2 protein (Fig. 5D). Thus, the PAX5 intermediate domain containing the octapeptide motif, nuclear localization sequence (NLS) and homeodomain is responsible for association with the RIP2 kinase domain, which might affect RIP2 phosphorylation.

We further explored whether PAX5-regulated RIP2 phosphorylation is involved in the RIP2-dominated NOD pathway. First, we found that NOD1 and NOD2 are expressed in IM9 cells (Fig. S2), which is consistent with previous reports (Lin

Journal of Cell Science (2016) 129, 2261-2272 doi:10.1242/jcs.183889

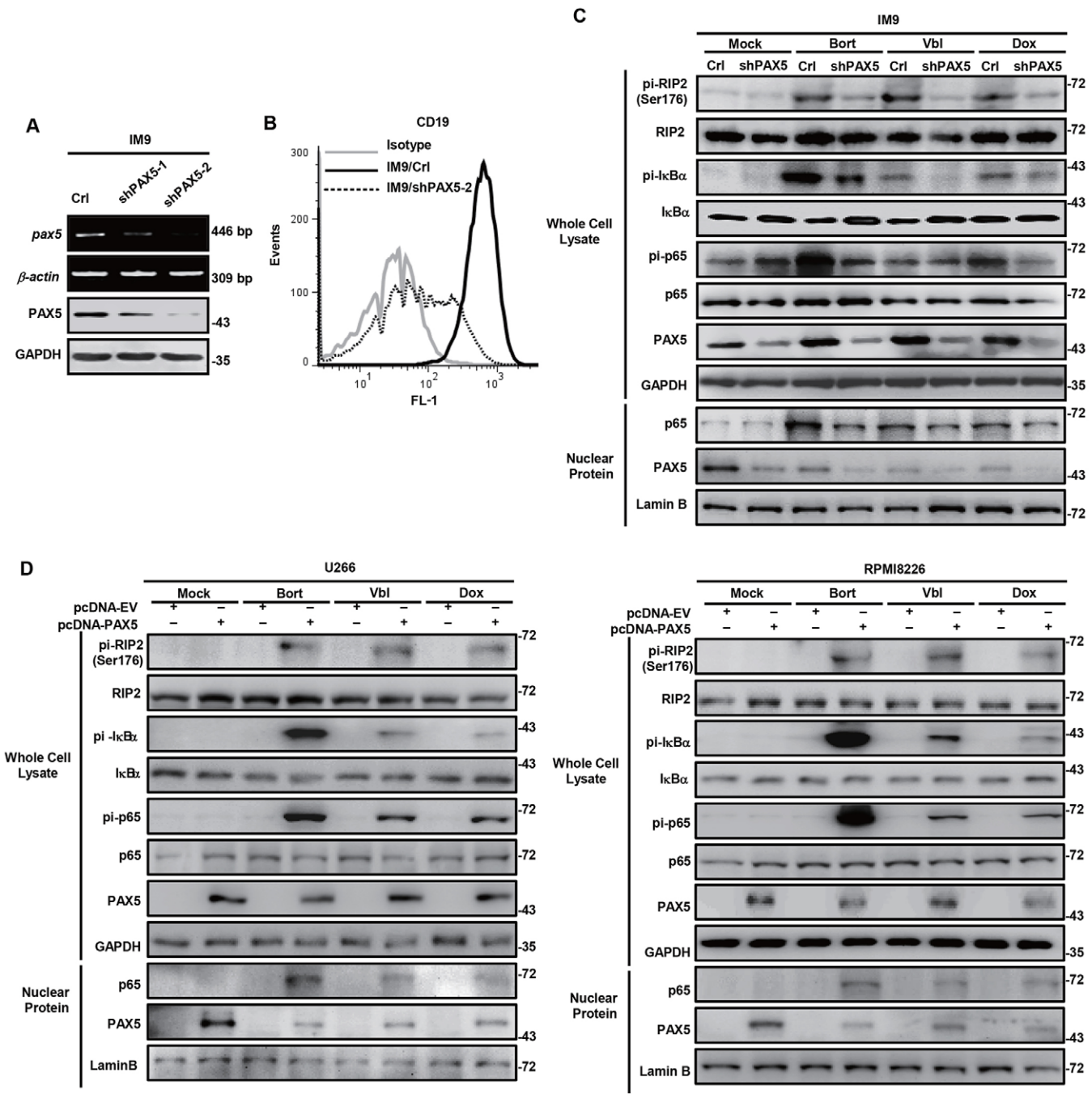

Fig. 2. PAX5 expression is related to drug-induced RIP2 and NF-κB activation. (A) Detection of *PAX5* expression in IM9-Crl cells and two different IM9-shPAX5 cell lines using RT-PCR (top two panels) and western blotting (bottom two panels). (B) Flow cytometry analysis of CD19 expression on IM9-Crl and IM9-shPAX5-2 cell surface. (C) IM9-Crl and IM9-shPAX5 cells were cultured in the presence or absence of Bortezomib (20 nM), Vinblastine (10 µg/ml) and Doxorubicin (10 µg/ml) for 4 h after serum starvation for 48 h. (D) U266 and RPMI8226 cells that had been transfected with pcDNA-Crl (pcDNA-EV) or pcDNA-PAX5 were cultured in the presence or absence of Bortezomib (20 nM), Vinblastine (10 µg/ml) and Doxorubicin (10 µg/ml) for 4 h. NF-κB activation and nuclear p65 were examined by western blotting. Data are representative of three independent experiments. Crl, control; Pi-, phosphorylated protein.

et al., 2013; Petterson et al., 2011). We employed the selective NOD1 and NOD2 agonists γ-D-Glu-mDAP (iE-DAP) and muramyl dipeptide (MDP) to stimulate IM9-Crl and IM9-shPAX5 cells, as well as HEK293T cells that expressed Flag–NOD1 and –NOD2. The results showed that iE-DAP- and MDP-induced activation of RIP2 and NF-κB were positively related to PAX5 expression (Fig. 5E and F), further confirming that PAX5 regulates RIP2 activation.

PAX5 impacts TNF-α-induced NF-κB activation through RIP1

Considering that PAX5 can interact with RIP1, PAX5 might be involved in RIP1 activity that is induced by TNF-α (also known as TNF). As shown in Fig. 6A, TNF-α-induced RIP1 ubiquitylation and NF-κB activation were substantially attenuated when *PAX5* was knocked down in IM9 cells. Consistently, *PAX5* knockdown markedly reduced TNF-α-induced nuclear NF-κB binding (Fig. 6B), recruitment of p65 to the *ICAM1* promoter (Fig. 6C)

Journal of Cell Science (2016) 129, 2261-2272 doi:10.1242/jcs.183889

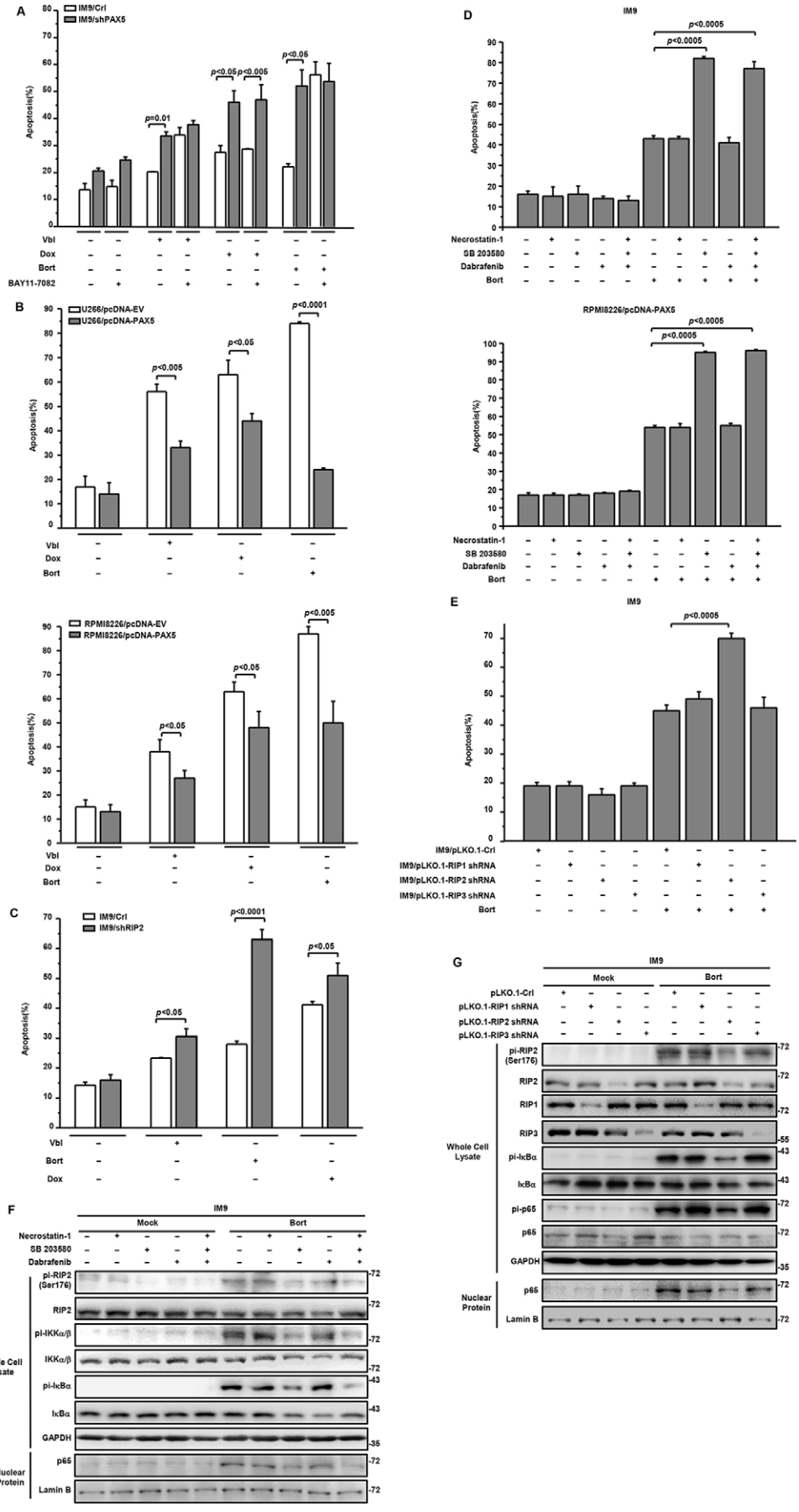

Fig. 3. PAX5 induces drug resistance by promoting NF-κB activation. Apoptosis assay. The indicated cells were treated with Bortezomib (Bort, 10 nM), Doxorubicin (Dox; 1 μg/ml) or Vinblastine (Vbl; 1 μg/ml) for 30 h in the presence or absence of 5 nM BAY11-7082 for IM9-Crl and IM9-shPAX5 (A), as well as in the absence of BAY11-7082 for U266 and RPMI8226 cells that had been transfected with pcDNA-Crl or pcDNA-PAX5 (B) and IM9-Crl and IM9-shRIP2 (C). (D) IM9 and RPMI8226 cells expressing PAX5 were treated with Bortezomib (10 nM) for 30 h in the presence or absence of Necrostatin-1 (20 μM), SB203580 (10 nM) and Dabrafenib (10 μM). (E) IM9 cells that had been transfected with pLKO.1-Crl, pLKO.1-RIP1 shRNA, pLKO.1-RIP2 shRNA or pLKO.1-RIP3 shRNA were treated with Bortezomib (10 nM) for 30 h. Apoptosis (%) includes both Annexin-V^+ PI^+ and Annexin-V^+ PI^- cells. *P*-values, two-tailed Student's *t*-test. (F) IM9 cells were pretreated with Necrostatin-1 (20 μM), SB 203580 (10 nM) or Dabrafenib (10 μM), or in combination for 1 h after serum starvation for 48 h, following with Bortezomib (20 nM) stimulation for 4 h. (G) IM9 cells that had been transfected with pLKO.1-Crl, pLKO.1-RIP1 shRNA, pLKO.1-RIP2 shRNA or pLKO.1-RIP3 shRNA were treated with Bortezomib (20 nM) for 4 h. NF-κB activation and nuclear p65 were examined by western blotting. Data are representative of three independent experiments. Error bars, ±s.e.m. Crl, control; Pi-, phosphorylated protein.

Journal of Cell Science

Journal of Cell Science (2016) 129, 2261-2272 doi:10.1242/jcs.183889

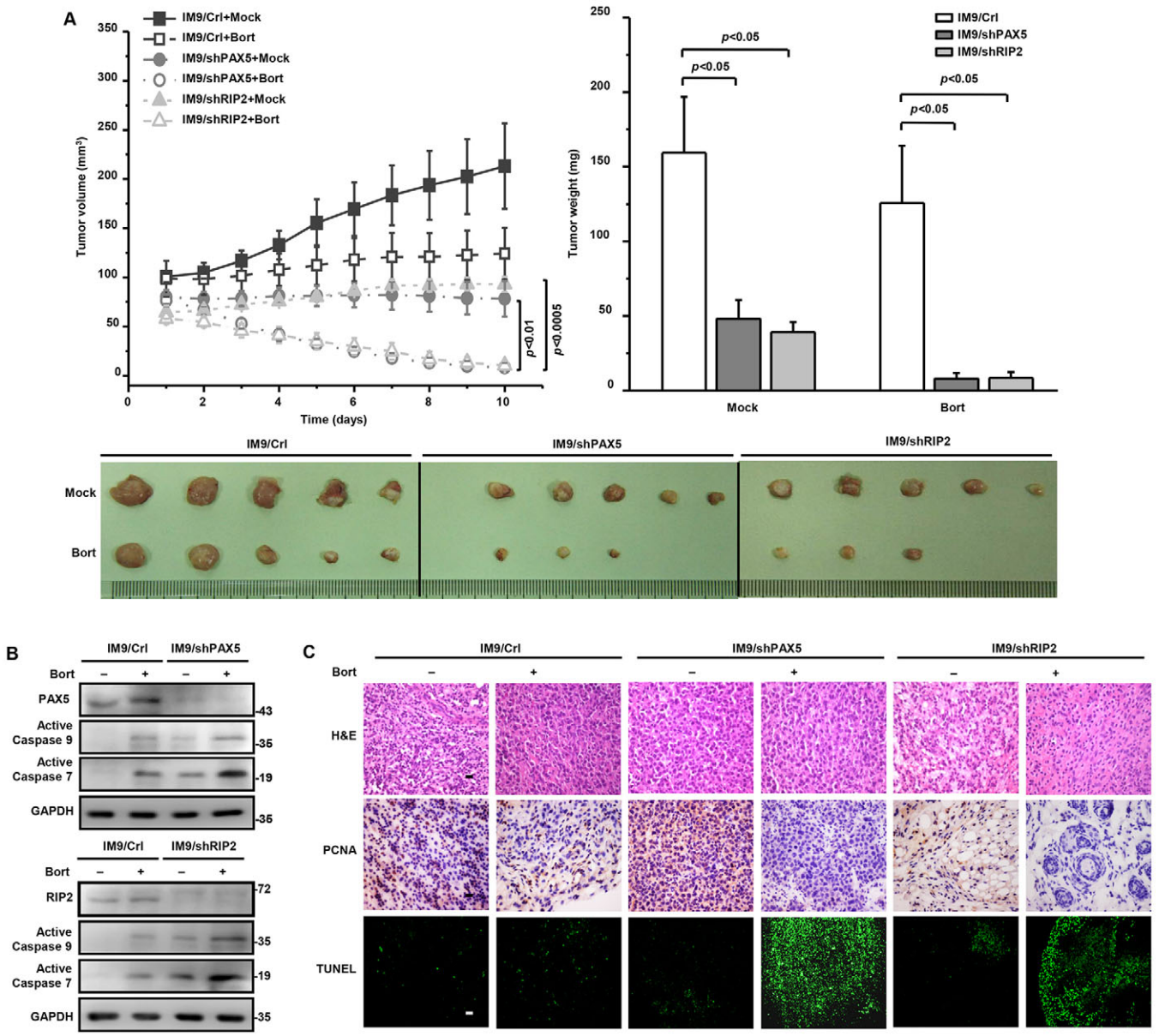

Fig. 4. PAX5 and RIP2 promote tumor growth and Bortezomib resistance *in vivo*. (A) A xenograft murine model was established with the indicated cells in nude mice. Tumor growth rate and tumor weight were measured, and photographs are shown. (B) Western blots for active caspase 7 and caspase 9 from tumors, as well as PAX5 and RIP2 expression. (C) Immunohistochemistry and TUNEL assays for tumor proliferation and apoptosis. Scale bars: 100 µm (TUNEL assay); 25 µm (immunohistochemistry). Error bars, ±s.e.m.; *P*-values, two-tailed Student's *t*-test. Data are representative of three independent experiments. Bort, Bortezomib.

and transcriptional activation of NF-κB target genes, including *BCL-XL*, *ICAM1* and *EGR1* (Fig. 6D) in IM9 cells. Altogether, these results reveal that PAX5 is also involved in RIP1-mediated NF-κB activation.

DISCUSSION

In response to stimuli, PAX5 associates with RIP2 and enhances RIP2 phosphorylation on Ser176, further elevating drug-induced NF-κB activation and promoting drug resistance (Fig. 7). It is well known that NF-κB activation contributes greatly to B-LPD pathogenesis (Jost and Ruland, 2007; Keller et al., 2006; Li et al., 2008; Strauss et al., 2006). NF-κB-associated protein mutations have been linked to canonical and non-canonical NF-κB abnormalities (Demchenko et al., 2010), and we found that high expression of PAX5 in B-LPDs indirectly caused NF-κB activation. Previous studies on PAX5 have been mostly focused on transcriptional regulation or cooperation with other tumor-associated proteins (O'Brien et al., 2011). In our model, PAX5 acts as an adaptor protein that might induce RIP2 conformational alterations that are prone to RIP2 autophosphorylation, which is followed by NF-κB activation. Moreover, it has been proven that NF-κB impacts B-lineage commitment by targeting *PAX5* expression (Balkhi et al., 2012). Therefore, we propose that a positive-feedback loop for *PAX5* expression and NF-κB activity might exist in B-cell differentiation. In addition, because the kinase domains that are responsible for interaction with PAX5 are highly conserved in RIP-family proteins (Zhang et al., 2010), PAX5 is also likely to interact with the kinase domains of other RIP-family members (RIP1, RIP3, etc.), regulating

Journal of Cell Science (2016) 129, 2261-2272 doi:10.1242/jcs.183889

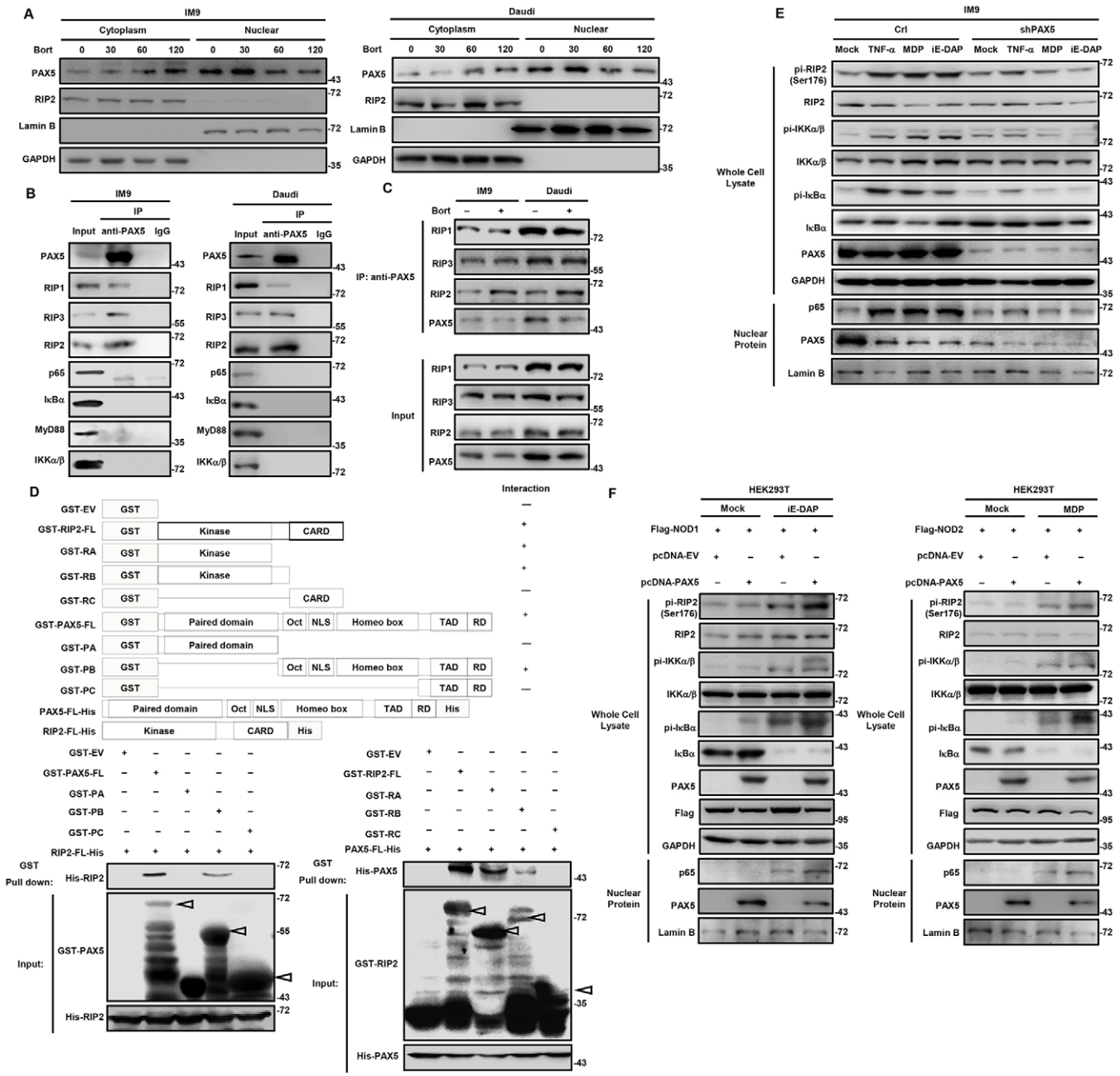

Fig. 5. PAX5 binds to RIP2 and affects the NOD–NF-κB pathway. (A) IM9 and Daudi cells were treated with Bortezomib (Bort; 20 nM) for 0, 30, 60 or 120 min. The distributions of PAX5 and RIP2 in the cytoplasm and nucleus were monitored by western blotting. GAPDH and lamin B are fractionation controls. (B) Coimmunoprecipitation analyses for PAX5-binding proteins in whole-cell lysates of unstimulated IM9 and Daudi cells. (C) IM9 and Daudi cells were cultured with or without Bortezomib (20 nM) for 2 h. Coimmunoprecipitation analyses for the binding of PAX5 to RIP1, RIP2 and RIP3. (D) GST-pulldown assay. Schematic diagram represents GST-tagged deletion constructs of RIP2 and PAX5 proteins. The summary of interactions of each domain in PAX5 and RIP2 proteins is indicated according to the results from the pulldown assay. Data are representative of three independent experiments. EV, empty vector; FL, full length; Oct, octapeptide motif; RD, repressor domain; TAD, transcription activation domain. Arrowheads indicate the full-length or truncated GST-tagged PAX5 and RIP2 proteins. (E) IM9-Crl and IM9-shPAX5 cells were cultured in the presence or absence of TNF-α (50 ng/ml) for 20 min, or MDP (100 ng/ml) or iE-DAP (100 ng/ml) for 30 min after serum starvation for 48 h. (F) HEK293T cells expressing Flag–NOD1 or Flag–NOD2 in combination with pcDNA-EV or pcDNA-PAX5 were cultured for 36 h before iE-DAP (100 ng/ml) or MDP (100 ng/ml) stimulation for 30 min. NF-κB activation and nuclear p65 were examined by western blotting. Data are representative of three independent experiments. Pi-, phosphorylated protein.

the activity of these RIP kinases and affecting multiple inflammatory signaling pathways, such as NOD and TNFR (Zhang et al., 2010). Moreover, whether RIP2 participates in TNFR signaling is still controversial, although it is interesting that RIP2 phosphorylation is increased in response to TNF-α treatment (Fig. 5D); however, it could be due to the specific cellular context in IM9 cells.

Bortezomib has been proven to trigger NF-κB activation by promoting RIP2 phosphorylation at Ser176, which is a new RIP2 autophosphorylation site identified to be an indicator of RIP2 activity (Hideshima et al., 2009; Dorsch et al., 2006). Phosphorylation at this residue might result from drug-induced ER stress, but clear understanding requires further investigation.

Journal of Cell Science (2016) 129, 2261-2272 doi:10.1242/jcs.183889

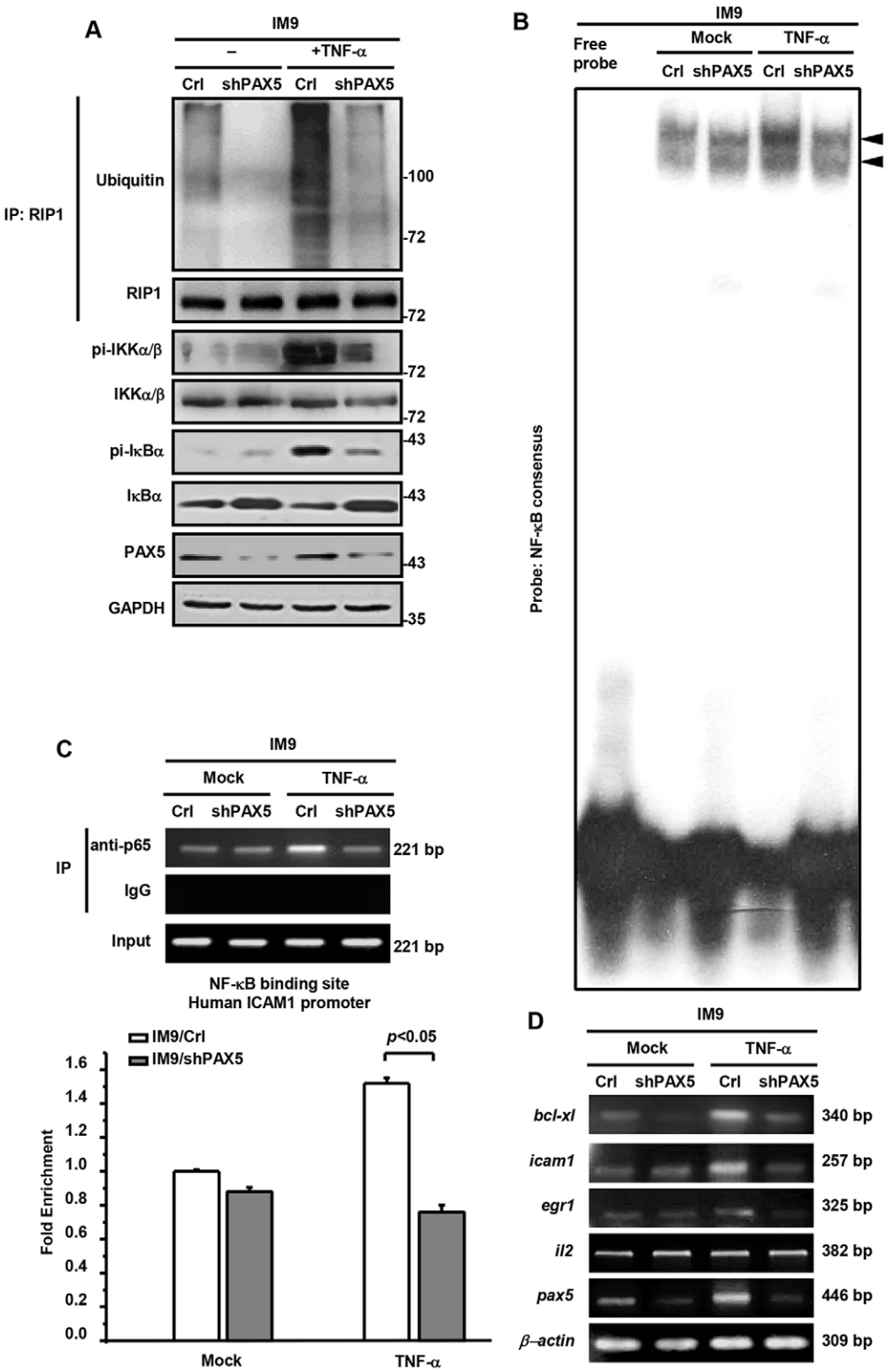

Fig. 6. PAX5 intensifies TNF-α-induced NF-κB pathways. (A) IM9-Crl and IM9-shPAX5 cells were cultured in the presence or absence of TNF-α (50 ng/ml) for 20 min after serum starvation for 48 h. RIP1 ubiquitylation and NF-κB activation were examined by western blotting. (B) IM9-Crl and IM9-shPAX5 cells were cultured in the presence or absence of TNF-α (50 ng/ml) for 20 min after serum-starvation for 48 h. The nuclear protein was extracted for analysis using an electrophoretic mobility shift analysis. Arrows indicate the specific NF-κB-probe-binding complexes. (C) Chromatin immunoprecipitation (ChIP) assay for p65 binding on the *ICAM1* promoter using PCR (upper panel) and real-time PCR (lower panel). (D) RT-PCR for *BCL-XL*, *EGR1*, *ICAM1*, *IL2* and *PAX5* mRNA detection in IM9-Crl and IM9-shPAX5 cells after serum-starvation for 48 h, followed by TNF-α (50 ng/ml) treatment for 12 h. Data are representative of three independent experiments. Crl, control; Pi-, phosphorylated protein.

Although overexpression of PAX5 has been reported to trigger non-drug-induced apoptosis in multiple myeloma cells (Proulx et al., 2010), our data suggest that PAX5 increases Bortezomib-induced NF-κB activation and drug-resistance by enhancing RIP2 Ser176 phosphorylation. Meanwhile, Bortezomib-induced apoptosis in primary multiple myeloma and leukemia cells has been proven to be related to PAX5 expression. Also, selective inhibitors and shRNAs against RIP1 or RIP3 fail to restrain Bortezomib-induced NF-κB activation and increase susceptibility of IM9 cells to Bortezomib, indicating that RIP1 and RIP3 are not involved in Bortezomib-induced drug resistance. Resistance to Bortezomib and Vinblastine results from elevated NF-κB activity, whereas resistance to Doxorubicin might be induced by other pathways involving PAX5. Unexpectedly, *PAX5* and *RIP2* knockdown impact the tumor-forming ability of IM9 cells *in vivo*. PAX5 inhibits CD80 and CD86 expression in IM9 (Fig. S3), which could serve as

Journal of Cell Science (2016) 129, 2261-2272 doi:10.1242/jcs.183889

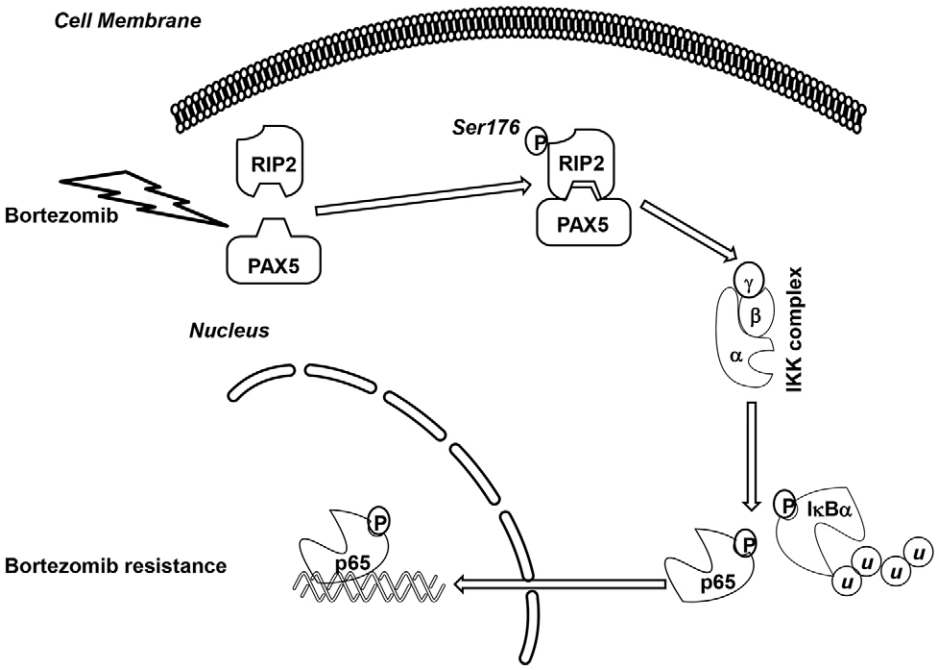

Fig. 7. A schematic model of a PAX5-regulated NF-κB pathway. Under drug or inflammatory stimulation, such as with Bortezomib, iE-DAP and MDP, PAX5 interacts with RIP2 and promotes phosphorylation at Ser176. RIP2 activation triggers the transduction cascade of the NF-κB pathway, including phosphorylation of IKK, IκBα and p65, as well as drug resistance. P, phosphorylation; u, ubiquitin.

costimulatory molecules for triggering natural-killer-cell-mediated cytotoxicity (Harnack et al., 2011; Luque et al., 2000; Wilson et al., 1999). RIP2 is also a crucial adaptor for the transmission of multiple signals and participates in the migration and invasion of breast cancer cells (Singel et al., 2014). These functions of PAX5 and RIP2 might affect the tumorigenic and apoptotic properties of IM9 cells in nude mice. Additionally, IM9-shPAX5 and IM9-shRIP2 tumors show higher sensitivity to Bortezomib *in vivo* than the control cells. These data suggest that PAX5 is a potential target for novel drugs and therapies.

In summary, PAX5 interacts with RIP2 and enhances RIP2 phosphorylation, leading to intensive NF-κB activity and drug resistance. These findings reveal a new function of PAX5 in drug resistance as well as its mechanisms of action in B-LPDs, indicate that PAX5 could be a new diagnosis marker and that it could be a valuable therapeutic target for PAX5-positive B-LPDs.

MATERIALS AND METHODS

Primary multiple myeloma and leukemia cell preparation

Written informed consent was obtained according to guidelines established by the Institutional Review Board of Anhui Medical University. The study was approved by the institutional ethics board of University of Science and Technology of China, and conducted in accordance with the Declaration of Helsinki. Bone marrow from multiple myeloma patients and peripheral blood from leukemia patients were processed using Ficoll-Paque gradient centrifugation. Primary tumor cells were purified (>95%) with CD138 (for multiple myeloma, n=11) or CD34 (for CD34-positive leukemia, n=8) positive selection using anti-CD138- or anti-CD34-antibody-conjugated magnetic activated cell sorting (MACS) microbeads (Miltenyi Biotec, Germany). Primary tumor cells were cultured with or without 5 nM Bortezomib for 30 h, followed by analysis of cell apoptosis. PAX5 expression was detected by performing reverse-transcription (RT)-PCR or immunohistochemistry analyses.

Cell lines

IM9, RPMI8226, U266 and Daudi cells were maintained in RPMI1640 medium with 10% FBS. HEK293T cells were maintained in Dulbecco's modified Eagle's medium with 10% FBS. The IM9 cell line is an Epstein-Barr virus (EBV)-transformed human B lymphoblast that is used as a representative malignant B-cell line. RPMI8226 and U266 cells are widely used multiple myeloma cell lines. Daudi cell line is Burkitt's-lymphoma-derived B lymphoblast (Torlakovic et al., 2006). IM9-Crl, IM9-shPAX5 and IM9-shRIP2 cells were obtained through transfection of plasmids expressing a scrambled sequence, and PAX5- and RIP2-specific shRNAs, respectively, into IM9 cells, and selected for drug-resistant lines. Selective shRNA sequences against *PAX5* and *RIP2* were: PAX5-shRNA-1, 5′-CTTGCTCATCAAGGTGTCATTCAAGAGATGACACCTTGATG-AGCAAGTTTTT-3′; PAX5-shRNA-2, 5′-CGGCCACTCGCTTCCGGG-CTTCAAGAGAGCCCGGAAGCGAGTGGCCGTTTTT-3′; RIP2-shRNA, 5′-CCGGGCACAATATGACTCCTCCTTTCTCGAGAAAGG-AGGAGTCATATTGTGCTTTTT-3′.

Plasmids and reagents

PAX5-specific shRNA sequences were inserted into pU6+27 vectors. Human RIP2 (RA, amino acids 1–310; RB, amino acids 1–454; RC, amino acids 455–540) and PAX5 (PA, amino acids 1–143; PB, amino acids 144–391; PC, amino acids 254–391) full-length and fragmental cDNA were subcloned into pGEX-4T-1. Full-length *PAX5* and *RIP2* cDNA were inserted into pET-22b. *PAX5* full-length cDNA was subcloned into pcDNA 3.0 vector. pLKO.1-RIP1, pLKO.1-RIP2 and pLKO.1-RIP3 shRNAs were purchased from Sigma-Aldrich. Selective shRNA sequences against RIP1 and RIP3 were: RIP1-shRNA, 5′-CCGGCCTTGTTGATAATGACTTCCACTCGAGTGG-AAGTCATTATCAACAAGGTTTTT-3′; RIP3-shRNA, 5′-CCGGCACA-GGGTTGGTATAATCATACTCGAGTATGATTATACCAACCCTGTGT-TTTT-3′. Human Flag–NOD1 and Flag–NOD2 expression vectors were obtained from Rongbin Zhou (School of Life Sciences, University of Science and Technology of China, Hefei, Anhui, China) as gifts.

The following reagents were used: Protein-A/G-plus–agarose (sc-2003, Santa Cruz Biotechnology); Bortezomib (B-1408, LC Laboratories); Doxorubicin and Vinblastine (D1515 and V1377, respectively, Sigma-Aldrich); BAY11-7082 (S1523, Beyotime Institute of Biotechnology, Shanghai, China); TNF-α (300-01A, Peprotech); Dabrafenib (M1988, Abmole, Houston, TX); MDP (53678-77-6, InvivoGen), iE-DAP (tlrl-dap; InvivoGen), SB 203580 (S1863, Beyotime Institute of Biotechnology) and Necrostatin-1 (480065, Millipore) were obtained from Rongbin Zhou as gifts.

Western blotting

Whole-cell and nuclear extracts were prepared as described in a previous study (Zheng et al., 2009). After SDS-PAGE separation, proteins were

Journal of Cell Science (2016) 129, 2261-2272 doi:10.1242/jcs.183889

transferred to PVDF membrane and incubated with antibodies, as indicated: anti-PAX5 (sc-1974X, 1:4000), anti-MyD88 (sc-74532, 1:1000), anti-p65 (sc-109X, 1:2000), anti-IKKα and -IKKβ (sc-7607, 1:1000) and anti-RIP3 (sc-374639, 1:1000) from Santa Cruz Biotechnology; anti-RIP1 (3493, 1:2000), anti-phosphorylated-RIP2 (Ser176) (4364, 1:2000), anti-phosphorylated-IKKα and -IKKβ (Ser176 and Ser180, respectively) (#2697, 1:2000), anti-phosphorylated-p65 (Ser536) (#3033, 1:2000), anti-phosphorylated-IκBα (Ser32) (#2859, 1:2000), anti-IκBα (#4812, 1:2000), anti-RIP2 (#4982, 1:1000), anti-GST (#2624, 1:2000), anti-cleaved-caspase-7 (#8438, 1:2000) and anti-cleaved-caspase-9 (#7237, 1:2000) from Cell Signaling Technology; anti-GAPDH (1105, 1:10,000) from KANGCHEN, Shanghai, China; anti-lamin B (BA36860, 1:1000) from BOSTER, Wuhan, China; anti-FLAG (F3165, 1:40,000) from Sigma-Aldrich; anti-His (#M20001, 1:10,000) from Abmart, Shanghai, China; anti-ubiquitin (AB24686, 1:4000) from Abcam, Cambridge, UK. Chemiluminescence was visualized using the ALLIANCE 4.7 chemiluminescence gel imaging system (UVItec, Cambridge, UK).

Reverse-transcription polymerase chain reaction

Total RNA was extracted using TRIzol reagent (Invitrogen). cDNA was synthesized using M-MLV reverse transcriptase according to the manufacturer's instructions. RT-PCR was performed, and products were visualized using a DNA gel imaging system (Tanon, Shanghai, China). Real-time PCR was performed using an ABI7500 instrument (Applied Biosystems) and the FastStart Sybr Green Master kit (Roche). Primers used in RT-PCR analyses were: human *PAX5*, forward 5′-ATCCGACTCCTCGGACCAGC-AGGAC-3′ and reverse 5′-ACTGGAAGCTGGGACTGGTTGGTTG-3′; human actin, forward 5′-GACCTGACTGACTACCTCATGAAGAT-3′ and reverse 5′-GTCACACTTCATGATGGAGTTGAAGG-3′; human *BCL-XL*, forward 5′-CGGGCATTCAGTGACCTGAC-3′ and reverse 5′-TCAGGA-ACCAGCGGTTGAAG-3′; human *EGR1*, forward 5′-CTGACCGCAGA-GTCTTTTCCTG-3′ and reverse 5′-TGGGTGCCGCTGAGTAAATG-3′; human *ICAM1*, forward 5′-TTCTCGTGCCGCACTGAACTG-3′ and reverse 5′-GAGTCGTTGCCATAGGTGACTG-3′; human *IL2*, forward 5′-AGTA-ACCTCAACTCCTGCCAC-3′ and reverse 5′-TTCAGATCCCTTTAGTT-CCAG-3′. Primers for real-time PCR: human *RIP1*, forward 5′-TGGGCG-TCATCATAGAGGAAG-3′ and reverse 5′-CGCCTTTTCCATGTAAGTA-GCA-3′; human *RIP2*, forward 5′-GCCCTTGGTGTAAATTACCTGC-3′ and reverse 5′-GGACATCATGCGCCACTTT-3′; human *RIP3*, forward 5′-AATTCGTGCTGCGCCTAGAAG-3′ and reverse 5′-TCGTGCAGGT-AAAACATCCCA-3′; human NOD1, forward 5′-ACTGAAAAGCAAT-CGGGAACTT-3′ and reverse 5′-CACACACAATCTCCGCATCTT-3′; human NOD2, forward 5′-CACCGTCTGGAATAAGGGTACT-3′ and reverse 5′-TTCATACTGGCTGACGAAACC-3′.

Flow cytometry

Cells were collected and blocked with 1% mouse serum, then washed after staining with FITC-conjugated anti-CD19 antibody (FHF019-010, 4A Biotech, Beijing, China), phycoerythrin-conjugated anti-CD80 antibody (305208, BioLegend), FITC-conjugated anti-CD86 antibody (555657, BD Biosciences) for 30 min. For cell apoptosis analyses, cells were incubated with FITC-conjugated anti-Annexin-V antibody (B157620, BioLegend) for 15 min, and then stained with propidium iodide. Samples were analyzed using a BD FACSCalibur instrument (BD Biosciences), and data processing was conducted using FlowJo software (Ashland, OR).

Electrophoretic mobility shift analysis

Nuclear protein was extracted using high-salt buffer (25 mM HEPES, pH 7.5, 10% sucrose, 0.01% NP-40, 1 mM DTT, 1 mM PMSF, 350 mM NaCl, 1 mM PMSF, 1 mg/ml leupeptin, 1 mg/ml pepstatin and 1 mg/ml aprotinin). An NF-κB consensus probe (Santa Cruz Biotechnology) was end-labeled with [γ^{32}P] adenosine triphosphate. Nuclear protein (3 µg) was incubated with an NF-κB consensus probe in binding buffer (12% glycerol, 12 mM HEPES pH 7.9, 1.5 mM $MgCl_2$, 60 mM KCl, 0.2 mM EDTA pH 8.0, 1 mM PMSF, 0.5 mM DTT and 0.5 µg poly deoxyinosinic-deoxycytidylic) for 20 min. The binding reaction mixtures were loaded onto 6% polyacrylamide gel, transferred to filter paper and visualized using autoradiography.

Chromatin immunoprecipitation

Cells were processed according to a previously described protocol (Ren et al., 2014). Anti-p65 and normal rabbit IgG (Santa Cruz Biotechnology) antibodies were separately added into lysates. Real-time PCR was performed by using an ABI7500 instrument (Applied Biosystems) and FastStart Sybr Green Master kit (Roche). Human *ICAM1*-promoter-NF-κB, forward 5′-CTTCGTCACTCCCACGGTTA-3′ and reverse 5′-AACTCA-AGTCCTCCCTCTCC-3′.

Coimmunoprecipitation and ubiquitin detection

Protein was extracted gently using coimmunoprecipitation lysis buffer (50 mM Tris-HCl, pH 7.6, 120 mM NaCl, 1% NP-40, 1 mM EDTA, 1 mM PMSF, 1 mg/ml leupeptin, 1 mg/ml pepstatin and 1 mg/ml aprotinin). Addition of a deubiquitylase inhibitor (10 µM N-ethylmaleimide) and proteasome inhibitor (1 µM MG132) was required for ubiquitin detection. Lysates were incubated with antibodies overnight at 4°C after pre-clearing with protein-A/G-plus–agarose. Protein-A/G-plus–agarose was added, then centrifuged and washed in coimmunoprecipitation washing buffer (20 mM Tris-HCl, pH 7.6, 100 mM NaCl, 1 mM EDTA and 1 mM PMSF) or ubiquitylation washing buffer (20 mM Tris-HCl, pH 7.6, 1 M NaCl, 1 mM EDTA and 1% SDS). Results were analyzed by immunoblotting.

Pulldown assay

GST- or His-tagged fusion proteins were expressed in BL21 *E. coli* and extracted using supersonic lysis. GST-fusion protein was bonded to glutathione–Sepharose beads for 4 h following incubation with His-fusion protein for 6 h. Glutathione–Sepharose beads were collected and washed in washing buffer. Results were analyzed by immunoblotting.

Immunohistochemistry

Tumors were fixed in 10% formaldehyde for 24 h followed by paraffin embedding, then processed as described previously (Xu et al., 2011). Human anti-PCNA antibody (sc-25280, 1:100, Santa Cruz Biotechnology) was used for detection of PCNA.

TUNEL assay

Paraffin-embedded tumor tissues were prepared, and the TUNEL assay was performed using the *In Situ* Cell Death Detection Kit, Fluorescein (Roche), according to the manufacturer's instructions. The final results were analyzed by using fluorescence microscopy.

Xenograft murine model

Four-week-old female nude mice were commercially obtained from the Laboratory Animal Center of the Academy of Military Medical Sciences. Mice were injected subcutaneously with IM9-Crl, IM9-shPAX5 or IM9-shRIP2 cells (3×10^7) in 100 µl RPMI1640 and 100 µl Matrigel (BD Biosciences). After tumors became a measurable size, mice were randomly placed into two group – the control group received 0.9% sodium chloride (n=5), and the Bortezomib group received 1 mg/kg bortezomib (n=5) twice weekly through the tail vein. Tumor volume was measured daily using the formula (length×width^2)/2. Ten days later, animals were killed and tumors were removed, weighed and photographed. All animal studies were conducted according to protocols approved by the Animal Ethics Committee of University of Science and Technology of China.

Statistics

P-values were calculated using the two-tailed Student's *t*-test. Error bars indicate the s.e.m. of at least three independent experiments. ANOVA analysis was also used to analyze statistical significance.

Acknowledgements

We thank Rongbin Zhou for valuable suggestions.

Competing interests

The authors declare no competing or financial interests.

Author contributions

D.W., Z.T., B.Y., C.Y., W.X. and Z.Z. designed the experiments and proposed the final model. D.W. conducted all experiments with assistance from R.L. and F.F. for

flow cytometry analysis; J.C. for immunofluorescence; Y.G. and Y.Z. for plasmid constructions; M.J., H.X., M.C. and J.S. for western blotting and G.S. for the xenograft murine model. G.W. and Z.W. provided multiple myeloma patient samples and performed immunohistochemistry. The paper was written and modified by D.W., Z.T. and W.X.

Funding
This work was supported by funds from National Basic Research Program of China (Ministry Of Science And Technology Of The People's Republic of China) [grant numbers 2013CB944903 and 2012CB825800]; and National Natural Science Foundation Of China [grant numbers 81071683, 91029710 and 81272327] to W.X.

Supplementary information
Supplementary information available online at
http://jcs.biologists.org/lookup/suppl/doi:10.1242/jcs.183889/-/DC1

References
Balkhi, M. Y., Willette-Brown, J., Zhu, F., Chen, Z., Liu, S., Guttridge, D. C., Karin, M. and Hu, Y. (2012). IKK alpha-mediated signaling circuitry regulates early B lymphopoiesis during hematopoiesis. *Blood* **119**, 5467-5477.

Brien, G., Trescol-Bierriont, M.-C. and Bonnefoy-Bérard, N. (2007). Downregulation of Bfl-1 protein expression sensitizes malignant B cells to apoptosis. *Oncogene* **26**, 5828-5832.

Cazzaniga, G., Daniotti, M., Tosi, S., Giudici, G., Aloisi, A., Pogliani, E., Kearney, L. and Biondi, A. (2001). The paired box domain gene PAX5 is fused to ETV6/TEL in an acute lymphoblastic leukemia case. *Cancer Res.* **61**, 4666-4670.

Chu, J., Deng, Y., Benson, D. M., He, S., Hughes, T., Zhang, J., Peng, Y., Mao, H., Yi, L., Ghoshal, K. et al. (2014). CS1-specific chimeric antigen receptor (CAR)-engineered natural killer cells enhance in vitro and in vivo antitumor activity against human multiple myeloma. *Leukemia* **28**, 917-927.

Cobaleda, C., Schebesta, A., Delogu, A. and Busslinger, M. (2007). Pax5: the guardian of B cell identity and function. *Nat. Immunol.* **8**, 463-470.

Davis, C. C., Marti, L. C., Sempowski, G. D., Jeyaraj, D. A. and Szabolcs, P. (2010). Interleukin-7 permits Th1/Tc1 maturation and promotes Ex vivo expansion of cord blood T cells: a critical step toward adoptive immunotherapy after cord blood transplantation. *Cancer Res.* **70**, 5249-5258.

Degterev, A., Maki, J. L. and Yuan, J. (2013). Activity and specificity of necrostatin-1, small-molecule inhibitor of RIP1 kinase. *Cell Death Differ.* **20**, 366-366.

Demchenko, Y. N., Glebov, O. K., Zingone, A., Keats, J. J., Bergsagel, P. L. and Kuehl, W. M. (2010). Classical and/or alternative NF-kappa B pathway activation in multiple myeloma. *Blood* **115**, 3541-3552.

Dong, H. Y., Browne, P., Liu, Z. and Gangi, M. (2008). PAX-5 is invariably expressed in B-cell lymphomas without plasma cell differentiation. *Histopathology* **53**, 278-287.

Dorsch, M., Wang, A., Cheng, H., Lu, C., Bielecki, A., Charron, K., Clauser, K., Ren, H., Polakiewicz, R. D., Parsons, T. et al. (2006). Identification of a regulatory autophosphorylation site in the serine-threonine kinase RIP2. *Cell. Signal.* **18**, 2223-2229.

Esparís-Ogando, A., Alegre, A., Aguado, B., Mateo, G., Gutiérrez, N., Bladé, J., Schenkein, D., Pandiella, A. and San Miguel, J. F. (2005). Bortezomib is an efficient agent in plasma cell leukemias. *Int. J. Cancer* **114**, 665-667.

Goy, A., Younes, A., McLaughlin, P., Pro, B., Romaguera, J. E., Hagemeister, F., Fayad, L., Dang, N. H., Samaniego, F., Wang, M. et al. (2005). Phase II study of proteasome inhibitor bortezomib in relapsed or refractory B-Cell non-Hodgkin's lymphoma. *J. Clin. Oncol.* **23**, 667-675.

Harnack, U., Johnen, H. and Pecher, G. (2011). Natural killer cell line YT exerts cytotoxicity against CD86(+) myeloma cells. *Anticancer Res.* **31**, 475-479.

Hideshima, T., Ikeda, H., Chauhan, D., Okawa, Y., Raje, N., Podar, K., Mitsiades, C., Munshi, N. C., Richardson, P. G., Carrasco, R. D. et al. (2009). Bortezomib induces canonical nuclear factor-kappa B activation in multiple myeloma cells. *Blood* **114**, 1046-1052.

Jost, P. J. and Ruland, J. (2007). Aberrant NF-kappa B signaling in lymphoma: mechanisms, consequences, and therapeutic implications. *Blood* **109**, 2700-2707.

Kanteti, R., Nallasura, V., Loganathan, S., Tretiakova, M., Kroll, T., Krishnaswamy, S., Faoro, L., Cagle, P., Husain, A. N., Vokes, E. E. et al. (2009). PAX5 is expressed in small-cell lung cancer and positively regulates c-Met transcription. *Lab. Invest.* **89**, 301-314.

Keller, S. A., Schattner, E. J. and Cesarman, E. (2000). Inhibition of NF-kappa B induces apoptosis of KSHV-infected primary effusion lymphoma cells. *Blood* **96**, 2537-2542.

Keller, S. A., Hernandez-Hopkins, D., Vider, J., Ponomarev, V., Hyjek, E., Schattner, E. J. and Cesarman, E. (2006). NF-kappa B is essential for the progression of KSHV- and EBV-infected lymphomas in vivo. *Blood* **107**, 3295-3302.

Kozmik, Z., Wang, S., Dörfler, P., Adams, B. and Busslinger, M. (1992). The promoter of the Cd19 gene is a target for the B-cell-specific transcription factor Bsap. *Mol. Cell. Biol.* **12**, 2662-2672.

Kozmik, Z., Sure, U., Ruedi, D., Busslinger, M. and Aguzzi, A. (1995). Deregulated expression Of Pax5 in medulloblastoma. *Proc. Natl. Acad. Sci. USA* **92**, 5709-5713.

Krenacs, L., Himmelmann, A. W., Quintanilla-Martinez, L., Fest, T., Riva, A., Wellmann, A., Bagdi, E., Kehrl, J. H., Jaffe, E. S. and Raffeld, M. (1998). Transcription factor B-cell-specific activator protein (BSAP) is differentially expressed in B cells and in subsets of B-cell lymphomas. *Blood* **92**, 1308-1316.

Kubetzko, F. B. B., di Paolo, C., Maag, C., Meier, R., Schäfer, B. W., Betts, D. R., Stahel, R. A. and Himmelmann, A. (2004). The PAX5 oncogene is expressed in N-type neuroblastoma cells and increases tumorigenicity of a S-type cell line. *Carcinogenesis* **25**, 1839-1846.

Li, Z.-W., Chen, H. M., Campbell, R. A., Bonavida, B. and Berenson, J. R. (2008). NF-kappa B in the pathogenesis and treatment of multiple myeloma. *Curr. Opin. Hematol.* **15**, 391-399.

Li, J. X., Feng, J. M., Wang, Y., Li, X. H., Chen, X. X., Su, Y., Shen, Y. Y., Chen, Y., Xiong, B., Yang, C. H. et al. (2014). The B-Raf(V600E) inhibitor dabrafenib selectively inhibits RIP3 and alleviates acetaminophen-induced liver injury. *Cell Death Dis.* **5**, 11.

Lin, P., Mahdavy, M., Zhan, F. H., Zhang, H.-Z., Katz, R. L. and Shaughnessy, J. D. (2004). Expression of PAX5 in CD20-positive multiple myeloma assessed by immunohistochemistry and oligonucleotide microarray. *Mod. Pathol.* **17**, 1217-1222.

Lin, Z., Hegarty, J. P., John, G., Berg, A., Wang, Z., Sehgal, R., Pastor, D. M., Wang, Y., Harris, L. R., III, Poritz, L. S. et al. (2013). NOD2 mutations affect muramyl dipeptide stimulation of human B lymphocytes and interact with other IBD-associated genes. *Dig. Dis. Sci.* **58**, 2599-2607.

Liu, P., Xu, B., Li, J. and Lu, H. (2009). BAG3 gene silencing sensitizes leukemic cells to Bortezomib-induced apoptosis. *FEBS Lett.* **583**, 401-406.

Luque, I., Reyburn, H. and Strominger, J. L. (2000). Expression of the CD80 and CD86 molecules enhances cytotoxicity by human natural killer cells. *Hum. Immunol.* **61**, 721-728.

Min, H.-J., Cho, I.-R., Srisuttee, R., Park, E.-H., Cho, D. H., Ahn, J.-H., Lee, I.-S., Johnston, R. N., Oh, S. and Chung, Y.-H. (2009). Hexachlorophene suppresses beta-catenin expression by up-regulation of Siah-1 in EBV-infected B lymphoma cells. *Cancer Lett.* **276**, 136-142.

Mitsiades, N. (2002). Biologic sequelae of nuclear factor-kappa B blockade in multiple myeloma: therapeutic applications. *Blood* **99**, 4079-4086.

O'Brien, P., Morin, P., Ouellette, R. J. and Robichaud, G. A. (2011). The Pax-5 gene: a pluripotent regulator of B-cell differentiation and cancer disease. *Cancer Res.* **71**, 7345-7350.

Pahl, H. L. (1999). Activators and target genes of Rel/NF-kappa B transcription factors. *Oncogene* **18**, 6853-6866.

Petterson, T., Jendholm, J., Mansson, A., Bjartell, A., Riesbeck, K. and Cardell, L.-O. (2011). Effects of NOD-like receptors in human B lymphocytes and crosstalk between NOD1/NOD2 and Toll-like receptors. *J. Leukoc. Biol.* **89**, 177-187.

Pridans, C., Holmes, M. L., Polli, M., Wettenhall, J. M., Dakic, A., Corcoran, L. M., Smyth, G. K. and Nutt, S. L. (2008). Identification of Pax5 target genes in early B cell differentiation. *J Immunol.* **180**, 1719-1728.

Proulx, M., Cayer, M.-P., Drouin, M., Laroche, A. and Jung, D. (2010). Overexpression of PAX5 induces apoptosis in multiple myeloma cells. *Int. J. Hematol.* **92**, 451-462.

Ren, Z., Kang, W., Wang, L., Sun, B., Ma, J., Zheng, C., Sun, J., Tian, Z., Yang, X. and Xiao, W. (2014). E2F1 renders prostate cancer cell resistant to ICAM-1 mediated antitumor immunity by NF-kappaB modulation. *Mol. Cancer* **13**, 84-84.

Shimizu, T., Nakazato, T., Xian, M. J., Sagawa, M., Ikeda, Y. and Kizaki, M. (2006). Resveratrol induces apoptosis of human malignant B cells by activation of caspase-3 and p38 MAP kinase pathways. *Biochem. Pharmacol.* **71**, 742-750.

Singel, S. M., Batten, K., Cornelius, C., Jia, G., Fasciani, G., Barron, S. L., Wright, W. E. and Shay, J. W. (2014). Receptor-interacting protein kinase 2 promotes triple-negative breast cancer cell migration and invasion via activation of nuclear factor-kappaB and c-Jun N-terminal kinase pathways. *Breast Cancer Res.* **16**, R28.

Strauss, S. J., Maharaj, L., Hoare, S., Johnson, P. W., Radford, J. A., Vinnecombe, S., Millard, L., Rohatiner, A., Boral, A., Trehu, E. et al. (2006). Bortezomib therapy in patients with relapsed or refractory lymphoma: potential correlation of in vitro sensitivity and tumor necrosis factor alpha response with clinical activity. *J. Clin. Oncol.* **24**, 2105-2112.

Stuart, E. T., Kioussi, C., Aguzzi, A. and Gruss, P. (1995). Pax5 Expression correlates with increasing malignancy in human astrocytomas. *Clin. Cancer Res.* **1**, 207-214.

Torlakovic, E., Slipicevic, A., Robinson, C., DeCoteau, J. F., Alfsen, G. C., Vyberg, M., Chibbar, R. and Flørenes, V. A. (2006). Pax-5 expression in nonhematopoietic tissues. *Am. J. Clin. Pathol.* **126**, 798-804.

Utecht, K. N. and Kolesar, J. (2008). Bortezomib: a novel chemotherapeutic agent for hematologic malignancies. *Am. J. HealthSyst. Pharm.* **65**, 1221-1231.

Wilson, J. L., Charo, J., Martin-Fontecha, A., Dellabona, P., Casorati, G., Chambers, B. J., Kiessling, R., Bejarano, M. T. and Ljunggren, H. G. (1999). NK cell triggering by the human costimulatory molecules CD80 and CD86. *J. Immunol.* **163**, 4207-4212.

Xiang, Y., Remily-Wood, E. R., Oliveira, V., Yarde, D., He, L., Cheng, J. Q., Mathews, L., Boucher, K., Cubitt, C., Perez, L. et al. (2011). monitoring a nuclear factor-kappa B signature of drug resistance in multiple myeloma. *Mol. Cell. Proteomics* **10**, M110.005520.

Xu, B., Hua, J., Zhang, Y., Jiang, X., Zhang, H., Ma, T., Zheng, W., Sun, R., Shen, W., Sha, J. et al. (2011). proliferating cell nuclear antigen (PCNA) regulates primordial follicle assembly by promoting apoptosis of oocytes in fetal and neonatal mouse ovaries. *PLoS ONE* **6**, e16046.

Zhan, F., Huang, Y., Colla, S., Stewart, J. P., Hanamura, L., Gupta, S., Epstein, J., Yaccoby, S., Sawyer, J., Burington, B. et al. (2006). The molecular classification of multiple myeloma. *Blood* **108**, 2020-2028.

Zhang, D., Lin, J. and Han, J. (2010). Receptor-interacting protein (RIP) kinase family. *Cell. Mol. Immunol.* **7**, 243-249.

Zheng, C., Ren, Z., Wang, H., Zhang, W., Kalvakolanu, D. V., Tian, Z. and Xiao, W. (2009). E2F1 induces tumor cell survival via nuclear factor-kappa B-dependent induction of EGR1 transcription in prostate cancer cells. *Cancer Res.* **69**, 2324-2331.